Title
Anisotropic electronic and magnetic properties of the quasi-two-dimensional heavy-fermion antiferromagnet CeRhIn5

Journal
Physical Review B, 62(21)

ISSN
2469-9950

Authors
Cornelius, AL
Arko, AJ
Sarrao, JL
et al.

Publication Date
2000-12-01

DOI
10.1103/physrevb.62.14181

Anisotropic electronic and magnetic properties of the quasi-two-dimensional heavy-fermion antiferromagnet $CeRhIn_5$

A. L. Cornelius
Department of Physics, University of Nevada, Las Vegas, Nevada 89154-4002

A. J. Arko, J. L. Sarrao, M. F. Hundley, and Z. Fisk*
Materials Science and Technology Division, Los Alamos National Laboratory, Los Alamos, New Mexico 87545

(Received 2 June 2000)

We have used high pulsed magnetic fields to 50 T to observe de Haas–van Alphen oscillations in the tetragonal antiferromagnet $CeRhIn_5$, which has an enhanced value of the electronic specific heat coefficient $\gamma \gtrsim 420$ mJ/mol K^2. For $T<T_N$, the specific heat data at zero applied magnetic field are consistent with the existence of an anisotropic spin-density wave opening a gap in the Fermi surface. The low-temperature magnetization reveals a magnetic phase transition that appears to be first order in nature. Quantum oscillations, which are observed for $T<T_N$ when $B\|[100]$ and $B\|[001]$, reveal an anisotropic Fermi surface. The temperature dependence of the amplitudes of the quantum oscillations shows anomalous behavior for $B\|[001]$ as a maximum at $T^* \approx 1.2$ K is observed which we attribute to a gap opening in the anisotropic Fermi surface. The electronic and magnetic properties are anisotropic due to the quasi-two-dimensional crystal structure.

I. INTRODUCTION

$CeRhIn_5$ crystallizes in the quasi-two-dimensional (quasi-2D) tetragonal $HoCoGa_5$-type structure and displays antiferromagnetic (AF) ordering at $T_N \approx 3.8$ K. The electronic specific heat coefficient ($\gamma \geqslant 420$ mJ/mol K^2) determined for $T>T_N$ makes $CeRhIn_5$ a moderately heavy-fermion compound. The evolution of the ground states as a function of applied pressure, including a pressure-induced first-order superconducting transition at 2.1 K, is unlike any previously studied heavy-fermion system and is attributed to the quasi-2D crystal structure.[1] We have completed experiments in an attempt to understand the unusual electronic and magnetic properties of $CeRhIn_5$, and we find that the anisotropic crystal structure leads to a quasi-2D electronic and magnetic structure.

We have performed measurements on $CeRhIn_5$ of the magnetization and de Haas–van Alphen (dHvA) effect in pulsed magnetic fields extending to 50 T and specific heat in zero applied field. At the lowest temperature measured in the magnetic studies (~ 0.4 K), a field-induced spin-density-wave (SDW) transition is found to occur at $B_M \approx 2$ T. The large difference in the Fermi surface measured in the two different field configurations $B\|[100]$ and $B\|[001]$ indicates that the Fermi surface is anisotropic, as expected from the quasi-2D crystal structure. The effective masses of the carriers range from $m^* = 0.8m_e$ to $1.4m_e$ (where m_e the free electron mass) for $B\|[100]$ and $m^* = 5m_e$ to $12m_e$ for $B\|[001]$. These values of m^* are consistent with $\gamma_0 \approx 56$ mJ/mol K^2, the value of the electronic specific heat coefficient for $T<T_N$ which is the temperature range of the dHvA measurements. For $B\|[001]$, the dHvA amplitudes are observed to go through a maximum as a function of temperature at $T^* \approx 1.2$ K, corresponding to a gap opening in the Fermi surface.

We have observed similarities in the electronic properties of $CeRhIn_5$ and compressed $CeIn_3$. Considering the resemblance in the environment around the Ce atom in the two compounds, it is not surprising that there are similarities in the electronic and magnetic properties. Many of the results on $CeRhIn_5$ will be discussed in terms of past results on $CeIn_3$. However, it is necessary to consider the 2D nature of the crystal structure to explain the magnetic and electronic properties (particularly the gaps that are observed in the Fermi surface and specific heat measurements and the field-induced magnetic transition).

II. TECHNIQUES

Single crystals of $CeRhIn_5$ were grown using a flux technique described elsewhere.[2] Using a standard four-probe measurement, the residual resistivity ratio between 2 K and 300 K was found to be greater than 100 for all measured crystals, indicative of high-quality samples. A clear kink was observed in the resistivity at $T_N = 3.8$ K. The specific heat was measured on a small (~ 11.7 mg) sample employing a standard thermal relaxation method in a ^{3}He system. The magnetization and dHvA effect were measured using counterwound highly compensated pickup coils in pulsed magnetic fields up to 50 T at the National High Magnetic Field Laboratory, Los Alamos. Throughout the pulsed field experiments, the sample was immersed in a ^{3}He or ^{4}He environment in which the temperature could be varied between ~ 0.4 K and 4 K.

III. RESULTS

A. Crystal growth

The single crystals of $CeRhIn_5$ were typically rods with dimensions from 0.1 to 10 mm with the long axis of the rod along the [100] axis of the tetragonal crystal. The samples were found to crystallize in the primitive tetragonal

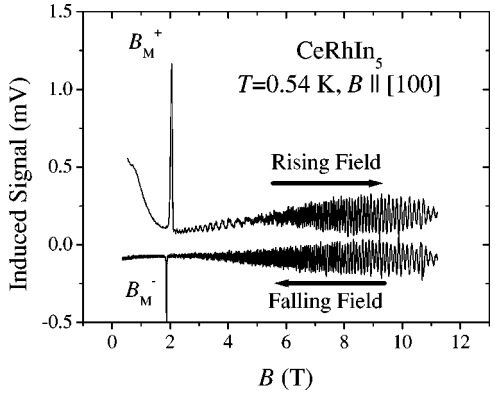

FIG. 1. The measured induced signal (voltage) vs applied pulsed magnetic field for $B\|[100]$ in $CeRhIn_5$ at 0.54 K. A magnetic transition is clearly observed at $B_M \approx 2$ T. Here B_M^+ and B_M^- correspond to the transition for rising and falling fields, respectively.

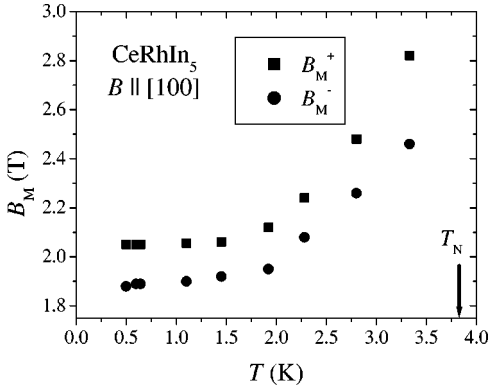

FIG. 2. The value of the magnetic transition field B_M^+ (rising field) and B_M^- (falling field) for $B\|[100]$ in $CeRhIn_5$ as a function of temperature.

$HoCoGa_5$-type structure[3,4] with lattice parameters of $a = 4.65$ Å and $c = 7.54$ Å, as evidenced by powder x-ray diffraction studies. The crystal structure of $CeRhIn_5$ can be viewed as $(CeIn_3)(RhIn_2)$ with alternating layers of cubic $(CeIn_3)$ and $(RhIn_2)$ stacked along the c axis. There is a single Ce site with $4/mmm$ symmetry. Taking the ambient pressure lattice parameter and the measured bulk modulus $B = 670$ kbar for $CeIn_3$,[5] the a lattice parameter, and therefore the Ce-Ce spacing, in $CeRhIn_5$ corresponds to $CeIn_3$ at 14 kbar. By looking at the crystal structure, we would expect that AF correlations will develop in the $(CeIn_3)$ layers just as they do in bulk $CeIn_3$.[6] The AF $(CeIn_3)$ layers will then be weakly coupled by an interlayer exchange interaction through the $(RhIn_2)$ layers which leads to a quasi-2D magnetic structure.

B. Magnetization

At $T_N = 3.8$ K, $CeRhIn_5$ is known to exhibit magnetic order.[1,7] The exact structure of the AF order is not known, but nuclear quadrupole resonance (NQR) measurements suggest that there is helical modulation that is incommensurate with the lattice and might be 2D in nature.[7] In Fig. 1, we show the measured inductive signal (which is directly proportional to dM/dH) versus magnetic field at 0.54 K for $B\|[100]$. A magnetic transition at $B_M^+ = 2.05$ T in rising field is clearly visible, with a small increase of the magnetic moment amounting to $\lesssim 0.006\ \mu_B$/Ce. In Fig. 2, the temperature dependence of B_M is shown for both rising (B_M^+) and falling fields (B_M^-). As can be seen, there is a clear hysteresis $(B_M^+ \neq B_M^-)$ between rising and falling fields which seems to increase as T approaches T_N. This leads us to conclude that the transition is first order in nature. In a simple model of a two-sublattice magnet applicable to what we expect for $CeRhIn_5$, a complicated phase diagram with many field-induced transitions of either first or second order can be realized.[8] Though this model treats both of the sublattices as having AF correlations (whereas only one sublattice would have AF correlations in $CeRhIn_5$), the general conclusions should be similar, and the model gives good qualitative agreement to the experimental results. The value of B_M rises as temperature is increased with a very rapid increase as T nears T_N. Typically one sees a decrease in the magnetic transition field as T increases for a magnetic-field-induced transition. The exact nature of the transition is unclear, but it is unlikely that it is truly a metamagnetic transition where one expects a drastic change in the character of the f electron which manifests itself as an increase in the magnetization on the order of 1 μ_B/Ce. However, the results are consistent with what is observed in quasi-1D and -2D SDW systems.[9,10] No transition was detected in the magnetization measurements for $B\|[001]$. These results lead us to conclude that the magnetic behavior can be explained by an anisotropic AF SDW that arises from a weak interlayer interaction between AF-ordered $(CeIn_3)$ blocks.

C. Heat capacity

The zero-field data from specific heat measurements are shown in Fig. 3. A peak at $T_N = 3.8$, indicating the onset of magnetic order, is clearly observed. The entropy associated with the magnetic transition is $0.3R \ln 2$ with the remaining $0.7R \ln 2$ recovered by 20 K. For $T > T_N$ the data could not be fit by simply using

$$C/T = \gamma + \beta_l T^2, \tag{1}$$

where γ is the electronic specific heat coefficient and β_l is the lattice Debye term. As found previously, one needs to

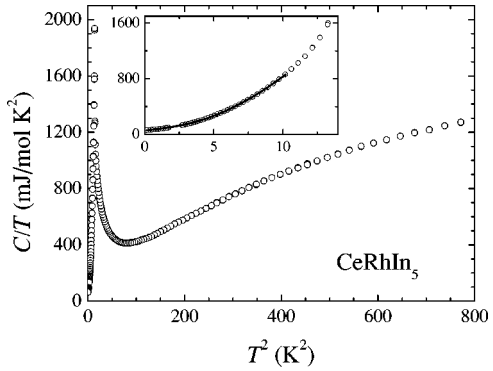

FIG. 3. The zero-field specific heat C divided by temperature T vs T^2 for $CeRhIn_5$. The inset displays the range $T^2 < 15$ K^2 corresponding to temperatures below T_N. The line is a fit as described in the text.

use isostructural, nonmagnetic $LaRhIn_5$ to subtract the lattice contribution to C.[1] Doing this leads to a value of $\gamma \gtrsim 420$ mJ/mol. As mentioned, the Ce-Ce separation of $CeIn_3$ at 14 kbar is identical to $CeRhIn_5$ at ambient pressure. Naively, one might expect that $\gamma(CeRhIn_5) \sim \gamma(CeIn_3$ at 14 kbar). From the high-pressure specific heat data on $CeIn_3$, an electronic Gruneisen parameter of $\Omega = 37$ is found.[11] Assuming that Ω is constant, this leads to an estimate for γ in $CeIn_3$ at 14 kbar of 310 mJ/mol K^2 which is in reasonable agreement with that of $CeRhIn_5$. This leads us to believe that the nature of the Ce-Ce interactions is similar in $CeIn_3$ at 14 kbar to $CeRhIn_5$ at ambient pressure.

If we look at temperatures below T_N, we expect that C/T can be approximated by an electronic term γ_0 and an AF magnon term $\beta_M T^2$. As can be seen in the inset to Fig. 3, the data for $T < T_N$ do not fall on a straight line, so the typical analysis cannot be used. This sort of behavior has been seen before in other Ce and U compounds where an additional activated term is needed to fit the data.[12–14] By using the form of Bredl[12] for the activated term, which arises from an AF SDW with a gap in the excitation spectrum due to anisotropy, we use the equation

$$C/T = \gamma_0 + \beta_M T^2 + \beta_M' (e^{-E_g/k_B T}) T^2 \tag{2}$$

to fit our $T < 0.85 T_N$ data where E_g is the activation energy. A fit to the data is shown in the inset to Fig. 3 using $\gamma_0 = 56 \pm 1$ mJ/mol K^2, $\beta_M = 24.1 \pm 0.4$ mJ/mol K^4, $\beta_M' = 706 \pm 16$ mJ/mol K^4, and $E_g/k_B = 8.2 \pm 0.1$ K. These values are similar to other Ce compounds that display this activated behavior.[12] In a two-band model of itinerant antiferromagnetism, it is found that the ratio of the gap energy to ordering temperature, or $E_g/k_B T_N$, should have a minimum value of 1.76. Our value of this quantity, $E_g/k_B T_N = 2.16$, is comparable to the calculated minimum value and similar to other measured gaps for systems with a SDW of 1.65 for YbBiPt,[15] 1.8 for $Ce(Ru_{0.85}Rh_{0.15})_2Si_2$,[14] 1.52 for URu_2Si_2,[13] and 2.3 for Cr.[16]

Though the agreement was not as good, the data could be fit reasonably with an empirical term, as done by many others,[14,17] added to the electronic term to give

$$C/T = \gamma_0 + A(e^{-E_g/k_B T})/T, \tag{3}$$

where A is a constant and E_g has a temperature dependence of the form $E_g = E_g(0)(1 - T/T_N)^{1/2}$. The best fit to our data gives a value of $E_g(0)/k_B = 9.6 \pm 0.2$ K. It has been pointed out, however, that this empirical form needs to be modified to take into account the dispersion of the magnetic excitation spectrum.[13] When this modification was performed on data taken on URu_2Si_2, the calculated gap was reduced from 129 K (Ref. 17) to 26.7 K (Ref. 13). Without a detailed neutron diffraction study to discern the magnetic dispersion, we feel that the results using Eq. (2) are more reliable.

The heat capacity results lead us to the conclusion that the magnetically ordered state in $CeRhIn_5$ consists of an anisotropic SDW that opens up a gap on the order of 8–10 K in the Fermi surface. From the ratio of the electronic contribution for temperatures above and below T_N, we estimate that approximately $\gamma_0/\gamma \sim 0.13$ of the Fermi surface remains ungapped below T_N.

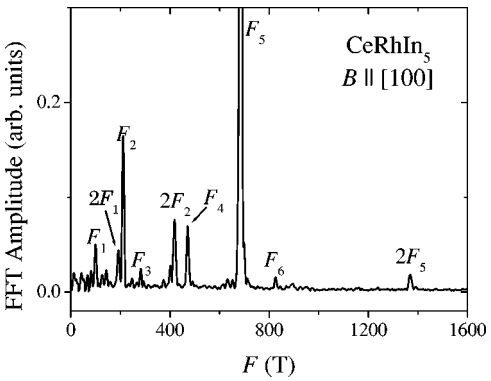

FIG. 4. The fast Fourier transform (FFT) amplitudes of the measured signal in Fig. 1 as a function of inverse applied field for $B \| [100]$. The peaks that appear in the FFT data labeled F_1–F_6 correspond to Fermi-surface orbits which have their physical properties summarized in Table I.

D. de Haas–van Alphen effect

The dHvA effect is the most definitive experimental probe of the Fermi surface properties of metals; the frequency of the oscillations F is directly proportional to extremal cross-section areas of the Fermi surface, while the amplitude of the oscillations yields important information concerning the electronic interactions. Much theoretical and experimental work has been done on the Fermi surfaces of heavy-fermion systems.[18–22] The main finding of the studies is that a Fermi-liquid description works but is characterized by a heavily renormalized effective mass m^* which can be determined from standard Lifshitz-Kosevich (LK) theory.

The dHvA measurements were performed on samples in the shape of a parallelepiped with typical dimensions of $0.8 \times 0.8 \times 5$ mm^3 with the long axis along the crystalline [100] axis. The measured induced signal for $CeRhIn_5$ versus applied field for $B \| [100]$ is displayed in Fig. 1. There is clearly an oscillatory dHvA signature in the data. The fast Fourier transform (FFT) of the measured signal from Fig. 1 when plotted as a function of the inverse magnetic field is shown in Fig. 4, and numerous peaks, corresponding to extremal Fermi-surface orbits and assorted harmonics, are observed. The frequencies of the six observed orbits labeled F_1–F_6 along with the corresponding values of m^* and T_D (for $B > B_M$), as determined by fitting to LK theory, are listed in Table I. The values of m^* and T_D listed in Table I are averages of the values obtained for rising and falling field data over the range 4 T $< B <$ 11 T.

TABLE I. Measured de Haas–van Alphen frequencies F, effective masses m^*, and Dingle temperatures T_D above the magnetic transition at B_M for $B \| [100]$ in $CeRhIn_5$. The frequencies F_1–F_6 correspond to the labeled peaks in Fig. 4.

	F (T)	m^* (m_e)	T_D (K)
F_1	100	1.36 ± 0.23	0.60 ± 0.06
F_2	210	0.99 ± 0.10	0.69 ± 0.11
F_3	282	0.93 ± 0.15	0.77 ± 0.18
F_4	471	0.72 ± 0.14	1.25 ± 0.06
F_5	683	1.17 ± 0.09	1.86 ± 0.05
F_6	824	1.31 ± 0.22	1.90 ± 0.03

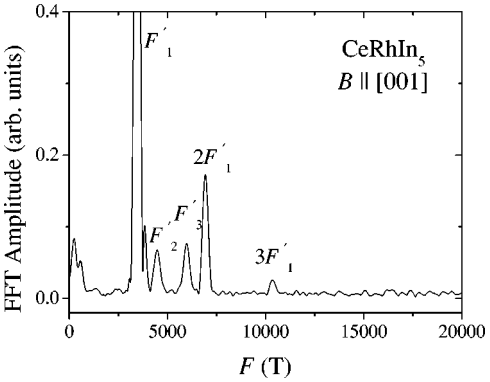

FIG. 5. The fast Fourier transform (FFT) amplitudes of the measured signal as a function of inverse applied field for $B\|[001]$. The peaks labeled F_1'–F_3' correspond to Fermi-surface orbits which have their physical properties summarized in Table II.

The FFT of the signal versus inverse magnetic field for $B\|[001]$ at $T=1.2$ K in the range 31 T$<B<$50 T is displayed in Fig. 5. Three orbits with frequencies labeled F_1'–F_3', along with assorted harmonics, are observed. The FFT amplitudes of the three orbits are plotted in Fig. 6 on a semilogarithmic plot as a function of temperature. The three amplitudes clearly display a maximum at $T^*\approx 1.2$ K. Since the maximum at T^* is seen for falling and rising fields and is observed after temperature cycling, and the temperature dependence of the Cu dHvA FFT amplitude (from the Cu pickup coils) is not anomalous, we conclude that the maximum at T^* is a real effect. For $T>T^*$, the amplitudes can be fitted using the standard LK formalism (the lines are fits using LK theory), and the frequencies F_1'–F_3' along with the corresponding values of m^* and T_D of the orbits are listed in Table II. For $T<T^*$, the amplitudes are seen to decrease in an exponential fashion, though we were unable to extract an accurate value for the gap from our data. This unusual behavior has been seen before in quasi-1D and quasi-2D materials; however, the oscillations in question in these studies were only seen in electric transport, not dHvA, measurements.[10,23–25] For one of these materials, it was determined that a gap opens in the electronic spectrum at the SDW transition temperature as determined from NMR measurements which display activated Korringa-like behavior

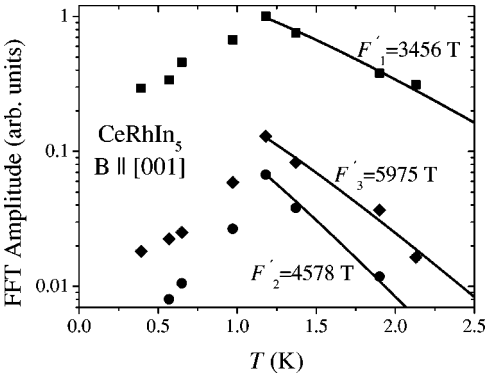

FIG. 6. The fast Fourier transform (FFT) amplitudes of the measured signal as a function of temperature for $B\|[001]$. The lines are fits as described in the text. All three orbits display a maximum at $T^*=1.2$ K.

TABLE II. Measured de Haas–van Alphen frequencies F', effective masses m^*, and Dingle temperatures T_D for $B\|[001]$ in $CeRhIn_5$. The frequencies F_1'– F_3' correspond to the labeled peaks in Fig. 5.

	F (T)	m^* (m_e)	T_D (K)
F_1'	3450	4.8 ± 0.4	0.75 ± 0.05
F_2'	4484	8.4 ± 1.0	1.26 ± 0.05
F_3'	5987	6.5 ± 0.8	2.41 ± 0.16

for $T<T_{SDW}$.[26] These results along with the analysis of the specific heat data point to $CeRhIn_5$ as having a gapped Fermi surface due to the formation of an anisotropic SDW.

The masses listed in Tables I and II appear to be rather low compared to the value of γ but are consistent with γ_0. Also, the dHvA masses and electronic specific heat coefficient are similar to those of bulk $CeIn_3$.[11,27,28] Because of this, we believe we are observing the entire Fermi surface of $CeRhIn_5$, though it is impossible to conclude this with absolute certainty.

Without a complete set of dHvA measurements as a function of the angle between the crystalline axes and magnetic field or a band structure calculation, it is impossible to say a great deal about the Fermi-surface topology. However, the great difference in the observed dHvA frequencies and masses for the two different orientations we measured indicates that there is clearly an anisotropy to the Fermi surface. Though it is tenuous to compare the Fermi surface of $CeRhIn_5$ to that of $CeIn_3$, we will proceed and take the results with caution. The dHvA frequency with the largest amplitude in $CeIn_3$ for $B\|[001]$ occurs at $F\approx 3300$ T with a mass of $m^*=2.3$.[27] If we assume that the only affect pressure will have on the Fermi surface is to increase m^*, this orbit is very similar to our measured largest orbit for $B\|[001]$ of $F_1'=3450$ T with $m^*=4.8$ for $CeRhIn_5$ at ambient pressure. While we have observed many more dHvA oscillations in $CeRhIn_5$ relative to $CeIn_3$ due to the more complicated crystal structure of $CeRhIn_5$, our choice of starting with compressed $CeIn_3$ to approximate the electronic structure of $CeRhIn_5$ again seems to have merit for $B\|[001]$. Perhaps the Fermi surface is cylindrical, reflecting the 2D nature of the crystal structure, with orbits for $B\|[001]$ that are approximately the same as in $CeIn_3$.

We also examined the dHvA data for any field or temperature dependences of the frequencies or the masses. In weak ferromagnets[29,30] and some heavy-fermion systems, notably UPt_3,[31,32] it is known that there can be a large field dependence of the dHvA frequencies due to spin-split bands. We did not observe such an effect in $CeRhIn_5$. We also did not observe any significant temperature dependence of the dHvA frequencies. Within the experimental uncertainty of our measurements, we could not discern any field dependence of m^*.

IV. CONCLUSION

In summary, we have observed dHvA oscillations in the quasi-2D heavy-fermion antiferromagnet $CeRhIn_5$. The magnetic and electronic properties of $CeRhIn_5$ can be well explained by postulating the formation of an anisotropic

SDW which opens a gap in the Fermi surface at low temperatures. From heat capacity measurements, we estimate that ~13% of the Fermi surface remains ungapped below the magnetic ordering temperature. The anisotropy is a result of the tetragonal crystal structure of $CeRhIn_5$ which consists of cubic ($CeIn_3$) blocks which are weakly interacting along the *c* axis through ($RhIn_2$) layers, and there is a great deal of similarity between $CeRhIn_5$ and compressed $CeIn_3$. Though more work is needed to obtain the full 3D Fermi surface, the results here shed light on the unusual magnetic and electronic structure of $CeRhIn_5$.

ACKNOWLEDGMENTS

The work at LANL was performed under the auspices of the U.S. Department of Energy, and the NHMHL is supported by the NSF and the state of Florida. One of us (A.C.) would like to acknowledge useful discussions with N. Harrison and support from DOE Cooperative Agreement No. DE-FC08-98NV13410.

*Also at National High Magnetic Field Laboratory and Department of Physics, Florida State University, Tallahassee, FL 32306.

[1] H. Hegger, C. Petrovic, E. B. Moshopoulou, M. F. Hundley, J. L. Sarrao, Z. Fisk, and J. D. Thompson, Phys. Rev. Lett. **84**, 4986 (2000).
[2] P. C. Canfield and Z. Fisk, Philos. Mag. B **65**, 1117 (1992).
[3] Y. N. Grin, Y. P. Yarmolyuk, and E. I. Gladyshevskii, Kristallografiya **24**, 242 (1979) [Sov. Phys. Crystallogr. **24**, 137 (1979)].
[4] Y. N. Grin, P. Rogl, and K. Hiebl, J. Less-Common Met. **121**, 497 (1986).
[5] I. Vedel, A. M. Redon, J. M. Mignot, and J. M. Leger, J. Phys. F: Met. Phys. **17**, 849 (1987).
[6] J. M. Lawrence and S. M. Shapiro, Phys. Rev. B **22**, 4379 (1980).
[7] N. J. Curro, P. C. Hammel, P. G. Pagliuso, J. L. Sarrao, J. D. Thompson, and Z. Fisk, Phys. Rev. B **62**, R6100 (2000).
[8] N. P. Kolmakova, S. A. Kolonogii, M. Y. Nekrasova, and R. Z. Levitin, Phys. Solid State **41**, 1649 (1999).
[9] P. M. Chaikin, E. I. Chashechkina, I. J. Lee, and M. J. Naughton, J. Phys.: Condens. Matter **10**, 11 301 (1998).
[10] P. Fertey, M. Poirier, and H. Muller, Phys. Rev. B **57**, 14 357 (1998).
[11] A. Berton, J. Chaussy, G. Chouteau, B. Cornut, J. Flouquet, J. Odin, J. Palleau, J. Peyrard, and R. Tournier, J. Phys. (Paris), Colloq. **40**, C5-326 (1979).
[12] C. D. Bredl, J. Magn. Magn. Mater. **63-64**, 355 (1987).
[13] N. H. van Dijk, F. Bourdarot, J. P. Klaasse, I. H. Hagmusa, E. Bruck, and A. A. Menovsky, Phys. Rev. B **56**, 14 493 (1997).
[14] S. Murayama, C. Sekine, A. Yokoyanagi, and Y. Onuki, Phys. Rev. B **56**, 11 092 (1997).
[15] R. Movshovich, A. Lacerda, P. C. Canfield, J. D. Thompson, and Z. Fisk, Phys. Rev. Lett. **73**, 492 (1994).
[16] E. Fawcett, Rev. Mod. Phys. **60**, 209 (1988).
[17] M. B. Maple, J. W. Chen, Y. Dalichaouch, T. Kohara, C. Rossel, M. S. Torikachvili, M. W. McElfresh, and J. D. Thompson, Phys. Rev. Lett. **56**, 185 (1986).
[18] A. Wasserman, M. Springford, and A. C. Hewson, J. Phys.: Condens. Matter **1**, 2669 (1989).
[19] M. Springford, Physica B **171**, 151 (1991).
[20] G. G. Lonzarich, J. Magn. Magn. Mater. **76-77**, 1 (1988).
[21] A. Wasserman and M. Springford, Adv. Phys. **45**, 471 (1996).
[22] L. Taillefer, J. Flouquet, and G. G. Lonzarich, Physica B **169**, 257 (1991).
[23] J. S. Brooks, J. O'Brien, R. P. Starrett, R. G. Clark, R. H. McKenzie, S. Y. Han, J. S. Qualls, S. Takasaki, J. Yamada, H. Anzai, C. H. Mielke, and L. K. Montgomery, Phys. Rev. B **59**, 2604 (1999).
[24] S. Uji, J. S. Brooks, M. Chaparala, S. Takasaki, J. Yamda, and H. Anzai, Phys. Rev. B **55**, 12 446 (1997).
[25] A. A. House, C. J. Haworth, J. M. Caulfield, S. J. Blundell, M. M. Honold, J. Singleton, W. Hayes, S. M. Hayden, P. Meeson, M. Springford, M. Kurmoo, and P. Day, J. Phys.: Condens. Matter **8**, 10 361 (1996).
[26] S. Valfells, P. Kuhns, A. Kleinhammes, J. S. Brooks, W. Moulton, S. Takasaki, J. Yamada, and H. Anzai, Phys. Rev. B **56**, 2585 (1997).
[27] R. Settai, T. Ebihara, M. Takashita, H. Sugawara, N. Kimura, K. Motoki, Y. Onuki, S. Uji, and H. Aoki, J. Magn. Magn. Mater. **140-144**, 1153 (1995).
[28] Y. Onuki and A. Hasegawa, in *Handbook on the Physics and Chemistry of Rare Earths*, edited by K. A. Gschneidner, Jr. and L. Eyring (North-Holland, Amsterdam, 1995), Vol. 20, Chap. 135, p. 1.
[29] T. I. Sigfusson, N. R. Bernhoeft, and G. G. Lonzarich, J. Phys. F: Met. Phys. **14**, 2141 (1984).
[30] J. M. Van Ruitenbeek, W. A. Verhoef, P. G. Mattocks, A. E. Dixon, A. P. J. Van Deursen, and A. R. de Vroomen, J. Phys. F: Met. Phys. **12**, 2919 (1982).
[31] N. Kimura, R. Settai, Y. Onuki, K. Maezawa, H. Aoki, and H. Harima, Physica B **216**, 313 (1996).
[32] S. R. Julian, P. A. A. Teunissen, and S. A. J. Wiegers, Phys. Rev. B **46**, 9821 (1992).